

# TRANSMISSION ELECTRON MICROSCOPY OF THE TEXTURED SILVER BACK REFLECTOR OF A THIN FILM SILICON SOLAR CELL: FROM CRYSTALLOGRAPHY TO OPTICAL ABSORPTION

M. Duchamp<sup>1</sup>, K. Söderström<sup>2</sup>, Q. Jeangros<sup>3</sup>, C.B. Boothroyd<sup>4</sup>, A. Kovács<sup>4</sup>, T. Kasama<sup>1</sup>, F.-J. Haug<sup>2</sup>, C. Ballif<sup>2</sup>, R.E. Dunin-Borkowski<sup>4,1</sup>

<sup>1</sup> Center for Electron Nanoscopy (CEN), Technical University of Denmark, DK-2800 Kongens Lyngby, Denmark

<sup>2</sup> Institute of Microengineering (IMT), Ecole Polytechnique Fédérale de Lausanne, CH-2000 Neuchâtel, Switzerland

<sup>3</sup> Interdisciplinary Center for Electron Microscopy (CIME), Ecole Polytechnique Fédérale de Lausanne, CH-1015 Lausanne, Switzerland

<sup>4</sup> Ernst Ruska-Centre and Peter Grünberg Institute, Research Centre Jülich, D-52425 Jülich, Germany

Phone: +45 45 25 64 70; email: martial.duchamp@cen.dtu.dk

**ABSTRACT:** The study of light trapping in amorphous, microcrystalline and micromorph thin-film Si solar cells is an important and active field of investigation. It has been demonstrated that the use of a rough Ag back-reflector lead to an increase of short circuit current but also to losses through the creation of surface plasmon polaritons. Here, we use transmission electron microscopy (TEM) techniques to study the grain structure of a Ag thin-film that was sputtered on top of 2- $\mu\text{m}$ -thick rough ZnO layer - defects, such as twin-boundaries have been observed. A smoothing of the top Ag surface was also observed after ex-situ annealing.

Electron energy-loss spectroscopy with a monochromatic beam was used to measure the surface plasmon resonance with nm spatial resolution. 1 eV and 3 eV Ag surface plasmon resonances have been observed on as-grown layers. Such measurements provide valuable information about the origin of optical absorption losses previously measured in Ag back-reflector of thin-film Si solar cells.

## 1 INTRODUCTION

The study of light trapping in thin-film Si solar cells is an important and active field of investigation [1]. A 45% improvement in current density has been predicted for an optimized back reflector structure in a microcrystalline thin film Si solar cell, when compared with the use of a flat reflector surface [2]. The most used route to control the light trapping is achieved using back and front contact texturation [3]. Nevertheless, the use of a rough Ag back reflector leads to higher optical absorption through the creation of extra surface plasmon polaritons [4-6]. A thin ZnO layer is therefore usually introduced between the Ag and the n-doped Si layers to limit plasmon absorption. Recently, standard cell characterization and optical measurements have shown an improvement in both external and internal quantum efficiency when an initially rough Ag layer is annealed at low temperature [5]. However, these measurements provide a global measure of absorption by the Ag layer but do not explain the origin of these optical losses.

Transmission electron microscopy (TEM) techniques can be used to study grain structure at the nanometre scale. In order to follow the evolution of defects during annealing, in-situ annealing experiments can be carried out. Moreover, combined with electron energy-loss spectroscopy (EELS), TEM has been used to excite localized surface plasmon on Ag nanotriangles [7]. It has been shown that Ag surface plasmon energies differ depending on the localization of the plasmonic excitation, i.e., lower energy being at the edge and higher energy at the centre of the nanoparticle. Moreover, the localization, the energy and the intensity of the Ag plasmon absorptions are of great interest in the field of solar cell as they are a source of parasitic absorptions, and so contribute to decrease the overall efficiency of the device.

## 2 EXPERIMENTAL DETAILS

### 2.1 Sample fabrication and ex-situ annealing

We used the pyramidal surface texture of 2  $\mu\text{m}$  thick LP-CVD ZnO grown on a 0.5-nm-thick glass substrate [8]. Then, 300 nm of Ag is deposited by DC sputtering (Univex 450B, Leybold, deposited at room temperature). The ex-situ annealed experiments of the Ag layer were carried out under air atmosphere at 150°C for 50 minutes.

### 2.2 TEM experimental setup

In-situ annealing and plasmon experiments are surface sensitive. In order to minimize the sample-preparation artefacts, we use conventional preparation techniques, i.e., 100-nm-thick-TEM specimens were obtained by polishing of original sample down to 20  $\mu\text{m}$ , and then milled with a low energy Ar beam and the final milling made at 500V.

Bright-field (BF), dark-field (DF) and selected-area-electron-diffraction (SAED) patterns were taken on an FEI Tecnai T-20 equipped with a LaB6 electron source. TEM in-situ annealing and EELS experiments were carried on an FEI Titan 80-300 equipped with a field emission electron source. In-situ experiments were carried out under  $\sim 1 \times 10^{-5}$  Pa vacuum in scanning (S)TEM mode, using 15 mrad inner angle angular-dark-field (ADF) detector (with such inner angle, the signal of the ADF detector is sensitive to the crystallographic diffraction of the sample as well as the mass projected to specimen thickness). The sample was kept for 30 minutes at the desired temperature before image acquisition was started. EEL spectra were acquired in STEM mode using a 74 mrad inner angle (the signal of the ADF detector is proportional to the atomic mass of the sample) with Gatan Tridiem electron-. Each spectrum was acquired for 20 seconds and the dispersion was 0.02 eV/pixel. In order to decrease the background contribution from the zero loss peak (ZLP), a 1 nm monochromated beam with a width at half maximum of  $\sim 0.2$  eV was used. EELS and in-situ experiments were carried out at 120 kV to minimise electron beam damage.

### 3 RESULTS and DISCUSSION

#### 3.1 As-grown and ex-situ annealing

The electrical and optical properties of a polycrystalline film are partly determined by the crystallographic features of the layer. In fact, the incident electro-magnetic field on a metal is mainly reflected if no defects are present, the optical absorption being caused by the exponential evanescent decay of the incoming field into the layer. When crystallographic defects are present, the light is scattered, following a Lambertian law. Determining the presence of defects, such as grain-boundaries or twin-boundaries, is important to understand the absorption/scattering of the light into the Ag back-reflector.

The first point to address when studying the optical absorption of an interface is the roughness of the interface. Fig 1 (a) and (b) show BF images of the as-grown and ex-situ annealed Ag layers. Both have a V-shape rough ZnO/Ag interface of period~300 nm and height 100 nm. The as-grown sample shows the same V-shape at the Ag/glue interface (in real device, ZnO replace the glue layer); in contrast, the ex-situ annealed sample has a much smoother top interface. This result has previously been observed on SEM cross-section with a larger field-of-view [9].

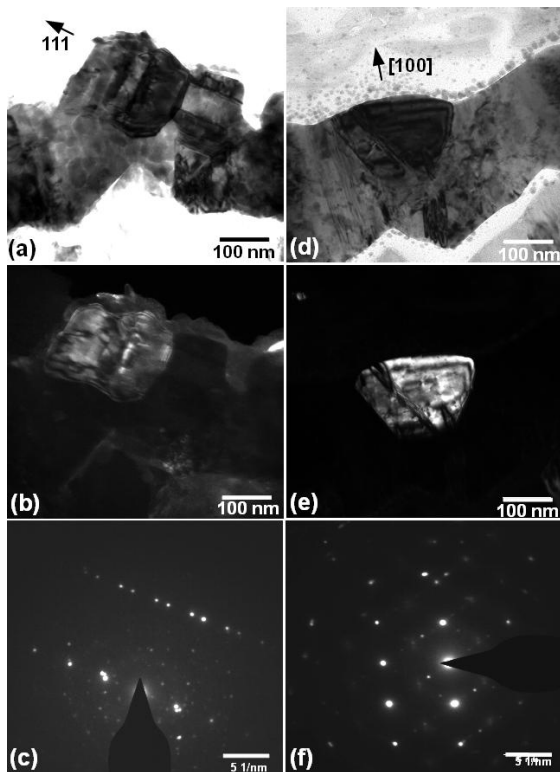


Fig 1: (a)-(d) bright-field, (b)-(e) dark-field TEM images and (c)-(f) SAED patterns from the Ag crystal shown in the dark-field images of Ag layers grown on a 2  $\mu\text{m}$ -thick ZnO buffer layer. (a-c) As-grown and (d-f) annealed at 150°C for 50 minutes in air.

Fig 1 (b) and (d) shows DF images of the two layers studied, the crystal size is about 100 by 100nm. The associated SAED patterns of the crystals observed in DF are shown in the insert. The extra spots in the as-grown diffraction pattern (fig 1 (b)) indicate the presence of twins. The twin-boundary surfaces are oriented

perpendicular to [111] preferred growth direction of the FCC Ag film (indicated in fig 1 (a)). After annealing, only a few twin-boundaries were observed (not shown), both on SAED pattern and BF images. The smoothing of the top interface and the decrease of the defect density could explain part of the decrease of the scatter reflectance and of the optical absorption of the annealed Ag layer, and therefore the increase the total reflectance.

#### 3.2 In-situ TEM annealing

In-situ TEM annealing allows us to track the heat-induced transformations of a given crystal. Fig 2 shows a series of STEM images obtained at different temperatures, from room temperature up to 210°C. The green arrow shows a small crystal with 10 by 10 nm in size, on the top surface of the Ag layer (according to the growth direction). This crystal size and location on the Ag layer may have a strong influence on the surface optical properties. Both the Ag/glue and Ag/Ag interfaces and the overall shape of this crystal do not seem to be affected by in-situ annealing. The red arrow shows a 100 nm long interface between two ~100 nm wide crystals located deeper into the layer. Such grain boundaries are suspected to scatter the incoming light. This grain-boundary seems to be unaffected by the low temperature anneal. On the other hand, the blue arrow shows a less defined interface. On annealing above 180°C this interface becomes sharper, which could be explained by both (i) a change of the interface orientation relative to the beam direction or (ii) by local recrystallisation.

In contrast to observations made during ex-situ annealing, the top surface stays rough during annealing. This could be due to the presence of glue on the top surface, which prevents the migration of Ag at its surface. The increase in optical reflectance after annealing could be related to the increase of the quality of the grain-boundaries. We also have to mention that the sample was exposed to a temperature of ~130 °C during sample preparation. One way to improve sample preparation and avoid ex-situ annealing would be to use focused ion beam (FIB) milling at low energies.

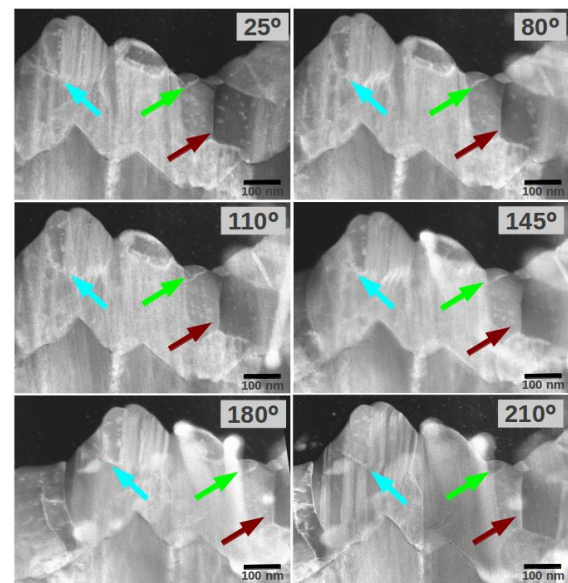


Fig 2: Series of STEM images of an in-situ Ag layer as it is annealed in-situ from 25 to 210 °C. The arrows show regions of interest (see text).

A second limitation due to sample preparation is the presence of glue on top of the layer, which could prevent Ag migration during annealing. In future experiments, a way has to be found to prepare TEM samples with the top surface exposed.

### 3.3 Methodology used to extract low-loss energy regions in EEL spectra

In the previous paragraphs, we presented the structural modifications that happened during low temperature annealing. In this section, we will try to find out (i) if plasmonic absorption can be observed in Ag thin-films using STEM-EELS and (ii) if they are involved in the surface optical absorption process. EEL spectra from two different regions of the as-grown sample, “bulk” and “surface”, were recorded. Figs 3 (a)-(d) shows the original 2D EEL images recorded on a CCD camera from the two regions marked in fig 4 (a). The vertical lines at the centre of the pictures are due to the slight difference in dark reference between the two quadrants of the CCD camera. 2D images rather than 1D spectrum are shown to present the method we used to remove the noise from the original data. Firstly, an efficient way to remove the noise is to use only the central part of the original spectrum (fig 3 (b)-(e)). Then, we apply principal component analysis (PCA) - which allows us to extract the components with the highest variance through an orthogonal transformation [10]. After applying PCA to the centre row of data, we obtained figs 3 (c)-(f), where peaks centred at  $\sim 4$  eV and,  $\sim 3$  eV are clearly visible.

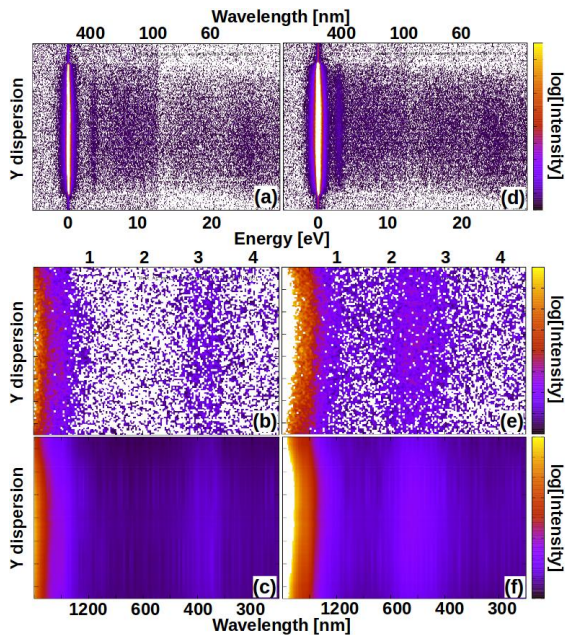


Fig 3: 2D EEL images (20 s exposure time) of (a-c) “bulk” and (d-f) “surface” regions of the Ag thin-film. See fig 4 (a) for the positions of the two regions. (a) & (d) A CCD camera of 2048 by 2048 pixels used during spectra acquisition. (b) & (e) centred as-acquired 2D spectra. (c) & (f) centred 2D spectra after removing noise using the PCA algorithm.

Fig 4 (b) shows the PCA filtered 2D spectra, figs 3 (c) & (f), summed along the y-direction. The signal from the “bulk” region clearly shows the Ag bulk plasmon peak at 3.8 eV. We also observe a shoulder at 1eV,

attributed to the surface plasmon from the entrance and exit surfaces of the electron beam. The spectra acquired at the edge of the Ag layer do not show the bulk plasmon peak. Instead they have a clear peak centred around 3 eV, which corresponds to a high surface plasmon mode. The peak at 1 eV is also present in this spectrum.

Previously, it has been demonstrated that the observed energy features in the EEL spectra are those of the electromagnetic eigenmodes of the nano-particles, the lower resonance energies being at the edge of the nanoparticles and the higher at the centre of the nanoparticles [8]. According to these previous measurements, the 1 eV peak measured in the “bulk” location is most probably due to the surface plasmon on the top and the bottom part of the layer. For the “surface” spectrum, the contribution of the 3 eV plasmon peak owes to a deeper area. Further, it has been shown that energy modes are size dependent, the energy decreases for increasing edge length of the nanoparticles. Söderström et al. have shown [5] that total reflectance is improved by annealing for energies lower than 1.2 eV, i.e., part of the spectrum for which surface plasmon contributions are predominant. Due to the broad range of crystal sizes, the plasmon resonance energy of the as-grown layer is also expected to be broader, and most probably covers all the energy range from 1 to 4 eV and becomes more intense for higher energy, as we observed that the 3 eV peak is broader and more intense than the low energy peak.

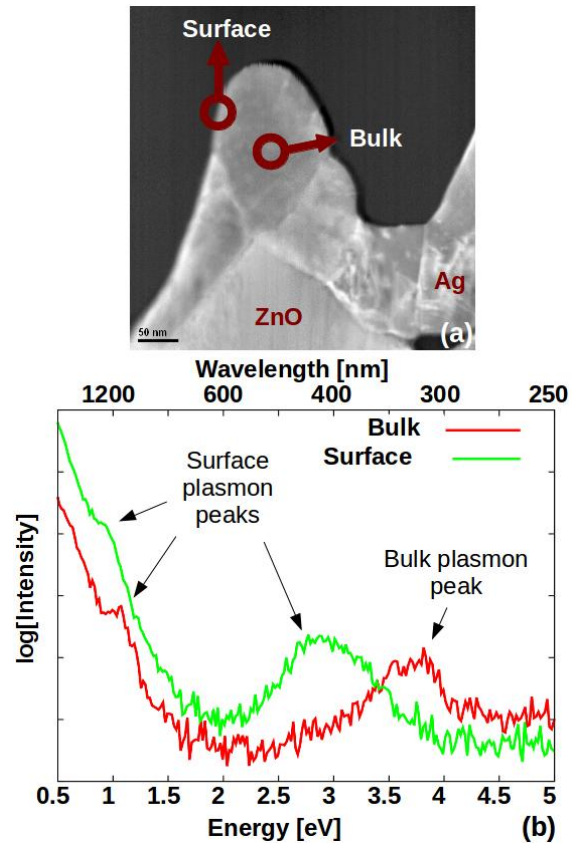


Fig 4: (a) STEM image of the as-grown Ag layer, the “bulk” and “surface” locations refer to the positions where the EEL spectra were recorded. (b) EEL spectra taken in the “bulk” and “surface” regions.

#### 4 CONCLUSIONS

We have studied the morphological transformations of the Ag layer used as a back-reflector in thin-film silicon solar cells. Previously, an improvement of the optical reflection for energies higher than 1 eV has been observed when rough Ag layers are annealed at  $\sim 150^\circ\text{C}$ . TEM images show a smoothing of the top Ag surface when ex-situ experiments are carried out in air. The presence of twin-boundaries have observed in as-grown crystals with fewer observed after ex-situ annealing. In-situ experiments have been carried out to follow the evolution of the grain structure, unfortunately, the sample preparation process and the presence of glue on top of the Ag layer seems to affect the sample both before and during in-situ annealing experiments.

To find out the origin of the optical losses, we performed EELS measurements on the edge and in the bulk part of the Ag layer. In order to remove the noise and extract the low intensity signal from the background contribution, we used a monochromated electron beam and performed PCA analysis directly on 2D spectra. The results clearly show the presence of a 1 eV surface plasmon peak in both the “bulk” and in the “surface” regions. In contrast, the 3 eV high mode surface plasmon peak was measured only at the edge of the layer and the 3.8 eV bulk plasmon peak only in the bulk part of the crystal. Such results show that we can measure the plasmon resonance with nm spatial resolution and a high enough energy resolution. Further experiments will be carried out to follow the evolution of plasmonic

absorption during in-situ experiments and to correlate the results with optical measurements made on bulk samples.

#### ACKNOWLEDGEMENTS

This work was financially supported by the EU (Silicon-Light project EU FP-7 Energy 2009-241477) and the Swiss National Science Foundation under grant no. 200021 12577/1.

#### REFERENCES

- [1] C. Rockstuhl et al., *Optics Express* 18 (2010) 129212
- [2] C. Andrej et al. *Journal of Applied Physics* 105 (2009) 083107
- [3] J. Müller et al., *Solar Energy* 77 (2007) 917
- [4] F.-J. Haug et al., *Journal of Applied Physics* 104 (2008) 064509
- [5] K. Söderström et al., *Solar Energy Materials and Solar Cells* (2011) submitted
- [6] V. Terrazzoni-Daudrix et al., *Progress in Photovoltaics: Research and Applications* 14 (2006) 485
- [7] J. Nelayah et al. *Nature Physics* 3 (2007) 348
- [8] S. Fay et al., *Solar Energy Materials and Solar Cells* 86 (2005) 385
- [9] K. Söderström et al. [MRS Online Proceedings Library, 1321](#), DOI:10.1557/opl.2011.812 (2011)
- [10] P. Trebbia et al. *Ultramicroscopy* 38 (1990) 165